Study of the mechanical properties of Ti-and Cr-based multicomponent hard coatings

Tetiana Cholakova[1,*], *Vasilliy* Chitanov[1], *Lilyana* Kolaklieva[1], *Roumen* Kakanakov[1], *Konstantin* Balashev[2], *Bogdan* Ranguelov[3], *Velko* Rupetchov[4] and *Georgi* Mishev[4]

[1]Central Laboratory of Applied Physics, Bulgarian Academy of Sciences, Plovdiv, Bulgaria
[2]Laboratory of Biophysical Chemistry, Department of Physical Chemistry, Sofia University, Bulgaria
[3]Institute of Physical Chemistry, Bulgarian Academy of Sciences, Sofia, Bulgaria
[4]Paisii Hilendarski University, Plovdiv, Technical College Smolyan, Bulgaria

Abstract. TiCrAlN and CrTiAlN multicomponent coatings have been developed using closed-field unbalanced magnetron sputtering technique (CFUBMS) in a gas mixture of Ar + N2. The nitrogen level was varied by using the feedback control of plasma optical emission monitor (OEM). An investigation into the effect of the CFUBMS process parameters on the properties of the coatings was undertaken. The main coatings parameters such as thickness, surface morphology, nanohardness, strength of adhesion and wear resistance were studied by means of ball-cratering method, atomic force microscopy, scanning electron microscopy, scratch tests and nanoindentation measurements. The study revealed strong dependency of the mechanical properties on the nitrogen flow rate. Analysis of the experimental results showed that Cr-based multicomponent coatings possess better mechanical properties than Ti-based coatings at a nitrogen flow rate of 21 sccm: higher value of hardness (≤ 31GPa) and higher scratch resistance (> 30 N).

1 Introduction

Unbalance magnetron sputtering technique was developed to improve the homogeneity of deposition films by increasing the region of homogeneous plasma and the substrate – target distance. This technique [1] has been used successfully to deposit various coating materials on different kind of substrates and tools. Hard coatings based on Ti and Cr nitrides are widely used as protective coatings. Cubic(c)-TiAlN and c-CrAlNcoatings have exhibited superior mechanical properties and oxidation resistance in comparison to traditional binary TiN and CrN coatings [2], and have been successfully used in the industry. Films based on the Ti-Cr-N system were also deposited using a variety of deposition methods in order to improve the hardness and wear resistance [3, 4]. Many studies were reported on the deposition and properties of TiAlN coating produced by various techniques. TiAlN coatings were developed by Physical vapour deposition (PVD) as an alternative to TiN, because of their higher oxidation resistance (>700°C), enhanced hardness (30–35 GPa) and higher corrosion resistance [5-10]. The later concept has been found to have promising

* Tetiana Cholakova: ipfban-dve@mbox.digsys.bg

performance compared to that of ternary films. Ti–Al–Cr–N system offers a high variability ranging from Cr rich to Al rich [11, 12] coatings. These films demonstrated improved hardness and thermal stability, oxidation resistance and exhibit lower friction and wear coefficient. However, as these coatings become more complex and the number of possible compositions increases dramatically, it is important to understand the role of each element in order to optimize the final composition, which determines their mechanical and tribological properties.

The present study focuses on the investigation of the Ti/TiN/TiAlCrN and Cr/CrN/CrTiAlN coatings obtained by a CFUBMS technique. The goal of this work is to establish optimal technological regimes which provide stable mechanical properties of the system "substrate - multicomponent coating" and to explore its potential for industrial application.

2 Experimental

2.1 Material and preparation

Ti-Cr-Al-N and Cr-Ti-Al-N coatings were deposited onto substrates of high-speed steel (HSS) and stainless steel (SS) using a closed-field unbalanced magnetron sputtering system UDP850 (Teer Coatings Ltd., UK) as shown in Figure 1. CFUBMS is equipped by four rectangular cathodes with high purity (99,99%) Cr, Ti and two Al targets operated in an unbalanced magnetron mode. The closed magnetic field coupling results in a highly degree of ionization and bias current density. Prior to the deposition, the substrates were cleaned in an ultrasonic bath for 5 min. at temperature of 65°C using commercial cleaning solution to remove oils, residues and protection against corrosion. After that the substrates were rinsed in distilled water for 2 min. followed by ultrasonic cleaning in hot isopropanol for 5 min. and dried up. Generally, ultrasonically cleaned metal substrates contain thin top oxide layer which affects the adhesion. After wet chemical cleaning the substrates were loaded in the deposition chamber and the system was pumped down to the base pressure less than $2{,}5\times10^{-3}$ Pa. In order to remove the top oxide layer the substrates were plasma cleaned in argon atmosphere ($1.7\text{x}10^{-1}$ Pa) for 30 min. at negative pulse substrate bias voltage of 500 V and frequency of 250 kHz. In all the deposition processes the substrates were biaxially rotated at a speed of 5 rpm in order to obtain homogenous film composition. The distance between the substrates and the targets was kept 150 mm.

All the experiments were realized without additional substrate heating at a bias voltage of -70 V and frequency of 150 kHz, in DC work regime of the Ti and Cr cathodes and pulsed regime of the Al cathodes. A mixture of argon and nitrogen gases was introduced into the chamber during the deposition process with a fixed Ar flow rate of 25 sccm. Nitrogen content was controlled by a plasma optical emission monitor with a feedback control of 95-50% (N_2 flow rate being in the range between 5 and 24 sccm).

Two series of experiments were performed under the same deposition conditions for deposition of Ti-based and Cr-based multicomponent coatings. In the first series, TiCrAlN coatings were deposited using Ti as the adhesive layer and TiN as an interlayer. In the second series, Cr and CrN were the adhesive layer and interlayer, respectively. Deposition started with a Ti or Cr adhesion layer. Over it a Ti-N or Cr-N transition film with gradually increasing nitrogen was layered. Following these two sub-layers, a compositionally graded Ti-Cr-Al-N or Cr-Ti-Al-N top layer was deposited. The relative concentration of Cr, Ti and Al in the coatings was adjusted through the sputtering power (P) applied to the targets during deposition: P_{Cr} = 1.5 kW; P_{Ti} = 2.4 kW; P_{Al} = 0.6 kW.

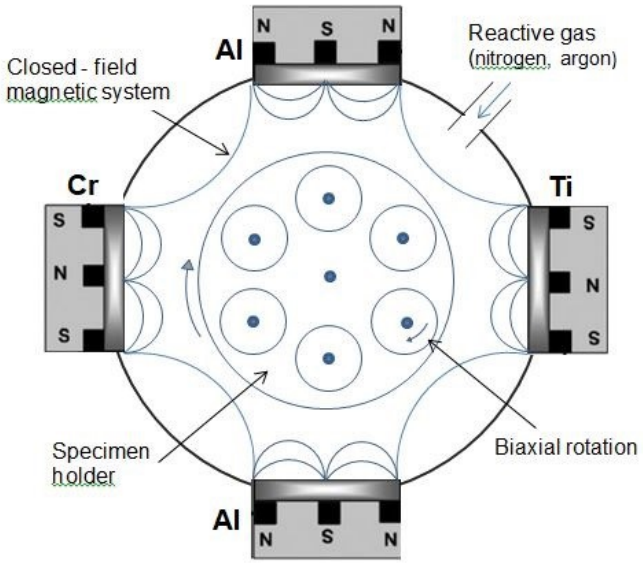

Fig.1. Cross-section schematic drawing of the CFUBMS sputtering system

2.2 Characterization

The coating thickness measurements were performed by a ball-cratering method (Calotest) which is suitable supplemental method providing information on configuration of individual layers and resistance to wear. Rotating ball of known diameter (20 mm or 30 mm) produces crater on the specimen surface, the so-called calotte which is used for determination the thickness of the layers.

Surface observations and morphology are performed on JEOL JSM 6390 electron microscope, equipped with INCA Oxford EDS energy dispersive detector. Surface images are obtained in secondary electrons (morphology contrast) and back-scattered electrons (density contrast) as well.

The Atomic force microscopy (AFM) studies were carried out by NanoScope VAFM (Bruker Inc.) in air in tapping mode. Silicon cantilevers with reflective aluminium coating with thickness of 30 nm, Tap 300Al-G (Budget Sensors, Innovative solutions Ltd, Bulgaria) were used. The characteristics of the cantilevers are as follows: spring constant, from 1.5 to 15 N/m, resonance frequency, 150 ± 75 kHz and radius of the tip curvature less than 10 nm. The scanning rate was set at 1 Hz.

The mechanical properties of the deposited coatings were investigated using Compact Platform CPX (MHT/NHT) CSM Instruments equipment which includes a Nanoindentation module (NHT), a Micro Scratch module (MST) and an Optical video microscope with CCD camera, installed together on the same platform. Nanoindentation was performed by a triangular diamond Berkovich pyramid in the loading interval of 10 - 200 mN.

The adhesion strength of the coatings to the substrate material and a friction coefficient were evaluated with MST equipped with a spherical Rockwell indenter with radius of 200 μm under the following test conditions: progressively increasing pressing force in a range of 1-30 N; loading rate 0.5 N/min; indenter movement speed 0.02 mm/min; acoustic emission detector sensitivity – 9. The character of the damages formed was assessed by observations with an Optical video microscope equipped with a CCD camera.

The wear resistance examinations were performed using a Ball on Flat Sliding Wear Test in a horizontal orientation of the test surface. A mineral-ceramic ball of Al_2O_3 with a diameter d = 3.0 mm, fixed in a holder, was used as a counter -body. The ball was rubbed on a Reciprocal Drive in air at room temperature, without lubricants**.**

3 Results and discussion

The study revealed that the same technological conditions have different effect on Ti –and Cr- based multicomponent coatings, which is, probably, due to different nucleation properties and growth rates during deposition. Below the results for the coatings deposited at a nitrogen flow rate of 21 sccm, which showed best mechanical properties, are presented.

3.1 Thickness and morphology

The thickness of the deposited coating was calculated from measurements of the diameters of the craters obtained in the coating and substrate using a steel ball with a diameter of 20 mm and diamond slurry with particles of 0.25 μm in diameter. The coating was abraded until the substrate was reached by the ball. This method provides an opportunity to observe continuous transition from layer to layer down to the substrate. The calculated total thickness (d) of deposited coatings is in the range of 1.8–2.5 μm. Figure 2a depicts architecture of the CrTiAlN coating, deposited at a nitrogen flow rate of 21 sccm.

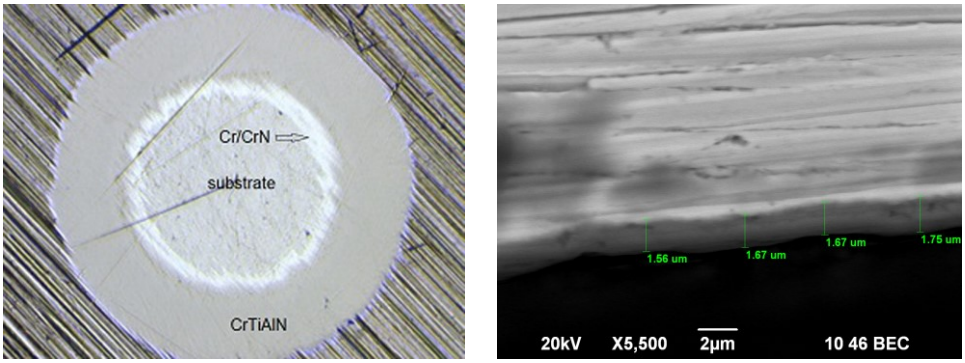

(a) **(b)**

Fig.2. An optical microscopy image of the CrTiAlN coating architecture, obtained by ball-cratering test (a) and the cross-sectional SEM micrograph (b) of same the coating sample

Determination of the coating thickness was performed also on a cross-section of the CrTiAlN coating using a scanning electron microscope (Fig.2b). The obtained result (d=1.75 μm.) is in good agreement with the Calotest method calculation (d=1.8 μm).

Several scans were performed by the AFM in tapping mode over different areas. The roughness analysis gives the value Ra, which is an arithmetic average of the absolute values Zj of the surface height deviations measured from the mean plane, while the image Rq is the root mean square average of height deviations taken from the mean image data plane. The AFM data revealed that the coating, obtained at a nitrogen flow rate of 21 sccm exhibited a densely packed structure [13], consisting of well separated grains with apparently spherical form and predominantly equal sizes (Fig.3a-b). The average roughness (Ra) and root mean square (Rq) surface roughness were obtained on a scanned area of 10 μm x 10 μm as follows: Ra = 16.4 nm and Rq = 22.0 nm. On the coating surface were

observed sporadic small defects, which lead to an increase of the roughness (Fig.3a, box): Ra=19.9 nm, Rq= 26.4 nm.

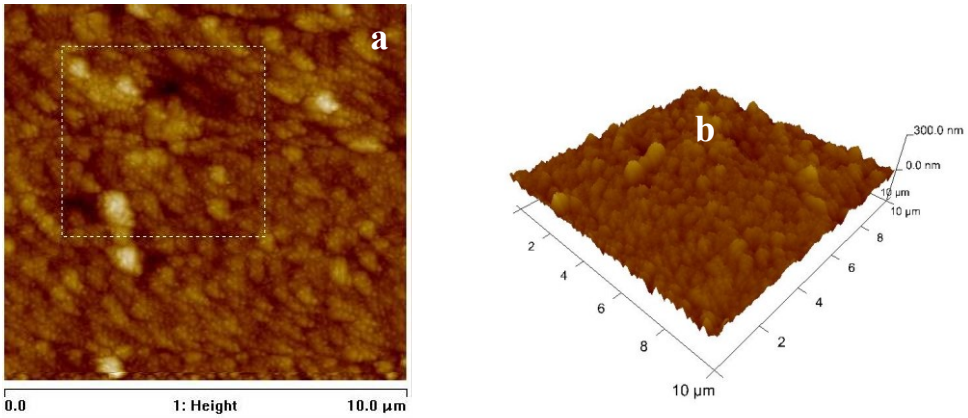

Fig.3. Surface topography of the CrTiAlN coating (SS substrate) obtained by AFM: a) 2D image - box dimension 5x5 µm; b) 3D image.

3.2 Hardness

The nanohardness (H) and elastic modulus (E) were calculated from nanoindentation load–displacement data at a periodic loading and unloading of the samples at a successively increasing load using an Oliver & Pharr method [14], executed by the software. To eliminate influence of the substrate on the measurement a load of 15 mN was applied, which corresponded to a maximum indentation depth of about 170 nm (less than 10% of the coating thickness). The maximum nanohardness of 31 GPa and elastic modulus of 418 GPa were measured for CrTiAlN coatings at the applied load of 15 mN. This value is higher as compared to the best value of the TiCrAlN coating (28 GPa and 358 GPa). The obtained nanohardness is significantly higher than those reported in [15, 16] and coincides with that obtained in [17].

3.3 Scratch strength

During the tests the load increased progressively in linear mode from 1N to 30 N at scratch lengths of 1 mm and 3 mm and constant scratch speeds of 0.02 mm/min and 0.05 mm/min. The measuring device registers the penetration depth and the acoustic emission along the length of the track. Three scratches on the coated HSS substrates for each sample were carried out in order to determine the adhesion strength. The critical load (*Lc*) values show relationship between the normal load, coefficient of friction and scratch length were determined after the test by optical microscopy observation of the damages formed in the scratch tracks and from the recorded acoustic emission (AE) and friction force (Ft) signals. The critical loads *Lc1* and *Lc2* indicate the appearance of the first cohesive and adhesive cracks, respectively [16].

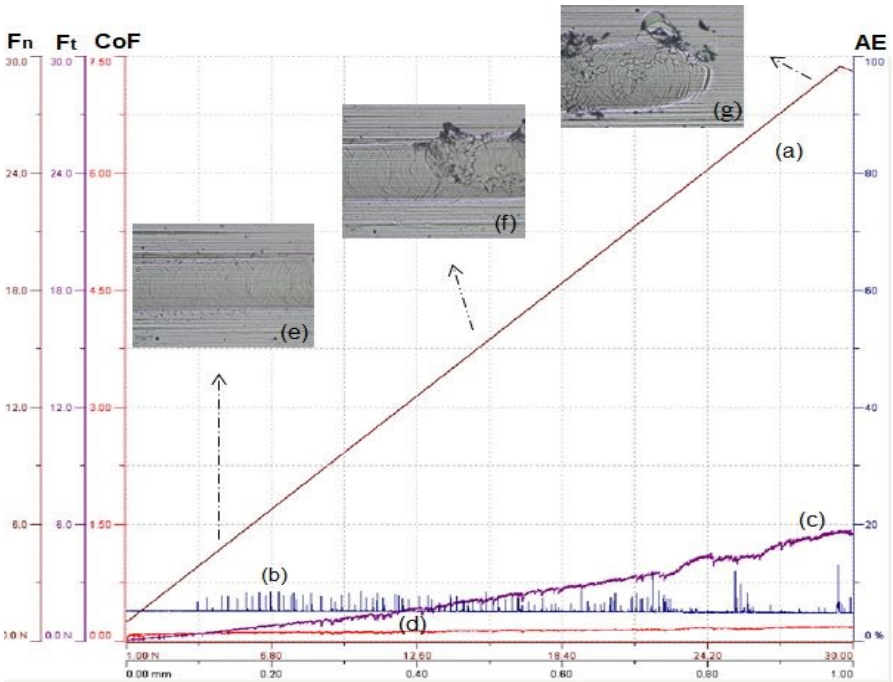

Fig.4. Typical scratch graphs on the TiCrAlN/HSS coating and optical micrographs (e, f and g) of the main parts of scratch track with cracks at different locations: a) Normal load; b) Acoustic emission; c) Friction force; d) Coefficient of friction.

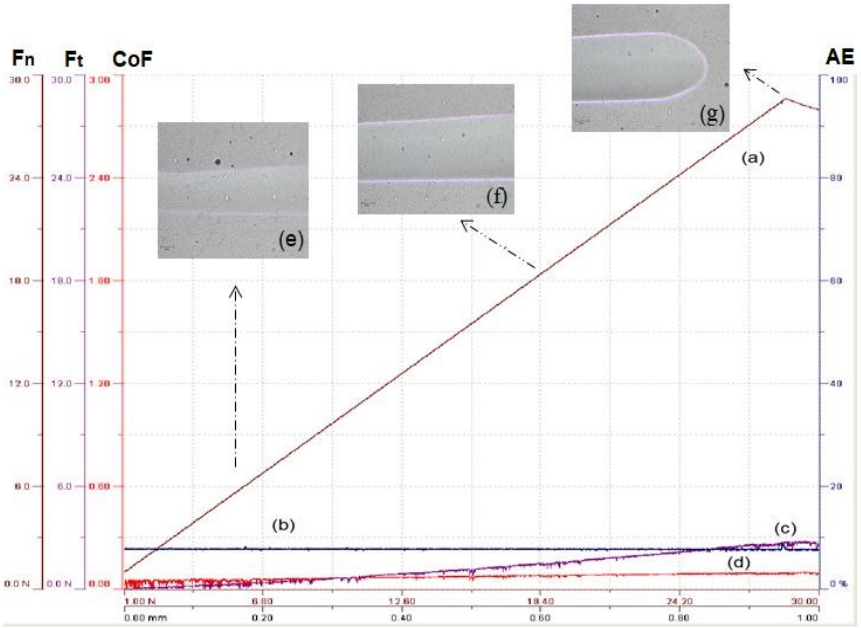

Fig.5. Typical scratch graphs on the CrTiAlN/HSS coating and optical micrographs (e, f and g) of the main parts of scratch track at different locations: a) Normal load; b) Acoustic emission; c) Friction force; d) Coefficient of friction.

The test consists of applying a continuously increasing load on the system coating-substrate at a constant speed. The scratching point causes increase the elastic and plastic deformation until damage occurs in the surface region. In most of the experiments the normal load at which the coating failure was initiated was detected by an increase in acoustic emission and confirmed by microscopic examination. Figure 4 shows scratch graphs of the TiCrAlN/HSS coating and the optical micrographs of the main parts of the scratch track with cracks at different locations. It is observed that with increase of the scratch length and the normal load respectively, the values of the friction force and acoustic emission are change. Very slight semi-circular cracks were observed at the normal load of about 5 N (Fig.4e). The first critical load is registered at Fn = 12,5 N (Fig.4f) and the second one at Fn = 23 N (Fig.4g). A distortion of the line of the friction force and the acoustic emission is observed at a higher normal load Fn = 23 N. However, it should be noted that the total removal of the coating did not occur within the loading interval.

The best adhesion result without any visible damages within loading range of 1-30 N possessed the CrTiAlN coating. An optical micrograph of the scratch track parts in the CrTiAlN coating and scratch test results of the acoustic emission (AE), friction force (Ft) and coefficient of friction (Cof), are shown in Figure 5.

As a result of the tests carried out, it was established that the critical loads Lc1 and Lc2 are observed for the Ti-based multicomponent coatings, while Cr-based coatings exhibit very good adhesion properties in the loading range 1 -30 N. The coefficient of friction of the Cr-based coatings against diamond indenter was measure to be μ= 0.1, while the Ti-based coatings had a higher coefficient of friction (μ ≈ 0.2).

3.4 Wear and wear rate

Investigations of the effect of normal force on the wear resistance of the CrTiAlN coating (d=2μm) at a load of 1, 1.5, 2, 2.5 and 3N and an average speed of sliding V_{av} = 20 mm/s = const. were carried out. The width of the groove was measured with a microscope TESA VISO-300 non-contact measuring system with magnification x100 (resolution 0.001 mm). The average value of the width of the groove (b_{av}) is determined by the equation:

$$b_{cp} = \frac{1}{n}\sum_{i}^{n} b_i \text{ , mm.} \quad (1)$$

The wear rate (coefficient) I_w was determined by the formula:

$$I_w = \frac{V}{F.L} \text{ , mm}^3\text{/N.m} \quad (2)$$

where: V is the volume of the removed coating material (track) in mm^3; F is the normal load in N; L is the sliding distance of the sample in m.

The track volume is determined according to the method described in [18, 19]. The wear coefficient is based on the assumption that the volume wear varies directly with the contact load and the sliding distance. The data of the wear volume and the wear rate as a function of the loading at V_{av} = 20 mm/s and L = 50 m are presented in Table 1.

The experimental results show that the normal load significantly influences on the wear of the Cr/CrN/CrTiAlN multilayer coating. The worn volume increases with the increase of the normal load while the wear intensity changes slightly. The experiments with loads from 1N to 3N passed completely in the coating without reaching the substrate. The maximum penetration depth (h) is 1.56 μm. It should be noted that the coating has a complex vertical construction (from the surface to the substrate) and, under greater load, it passes through

layers having different mechanical properties. Consequently, the volume variation at different loads is a direct criterion for the evaluation of the coating wear, while the wear rate I_w is an universally accepted measure for the wear of different coatings at the same working conditions.

Table 1: The calculated value of wear and wear rates of the CrTiAlN coating, deposited on an unhardened stainless steel substrate (1.2343).

F [N]	V x 10^{-6} [mm^3]	I_w x 10^{-6} [mm^3/N.m]	h x 10^{-3} [mm]
1	497.343	9.947	0.724
1.5	675.627	9.008	0.888
2	892.216	8.922	1.068
2.5	1128.545	9.028	1.249
3	1583.803	10.559	1.564

4 Conclusion

Two series of multicomponent coatings without additional substrate heating were successfully obtained under the same deposition conditions using the closed-field unbalanced magnetron sputtering technique. The study revealed strong dependency of the mechanical properties on the nitrogen flow rate. The coatings based on Ti/TiN/TiAlCrN and Cr/CrN/CrTiAlN exhibited hardness and an elastic modulus of 26 ± 5 GPa and 350 ± 70 GPa, respectively, at a nitrogen flow rate of 21 sccm. Further increase of the N_2 flow rate caused decreases of the coating hardness. The results of the scratch tests showed different states of adhesion to the HSS substrate of these coatings. The Cr-based coatings demonstrated excellent adhesion in the loading interval from 1N to 30N and a low coefficient of friction (μ=0.1), while the Ti-based coatings had worse adhesion expressed by presence of higher coefficient of friction (μ≈ 0.2) and a critical load Lc1 at loading of 12 N.

The research showed that further optimization of the deposition process of Ti-based multi-component coatings is needed in order to obtain better mechanical properties.

References

1. B.Window, N.Savvides, J.Vac.Sci.Technol. A, Vol. **4**, Iss.2, 196 (1986)
2. O.Knotek, M. Bohmer, T. Leyendecker, J. Vac. Sci. Technol. A, Vol. **4**, Iss. 6, 2695 (1986)
3. J.H. Hsieh, W.H. Zhang, C. Li, C.Q. Sun, Surf. & Coat. Technol., **146 –147**, 331–337 (2001)
4. W. Aperador, A. Delgado, J. C. Caicedo, Int. J. Electrochem. Sci., **12**, 4502 – 4514 (2017)
5. S. PalDey, S.C. Deevi, Mater. Sci. Eng. A, **342,** 58–79 (2003)
6. P.W. Shum, K.Y. Li, Z.F. Zhou, Y.G. Shen, Surf. & Coat. Technol., **185**, 245– 253 (2004)
7. S.K. Wu, H.C. Lin, P.L. Liu, Surf. & Coat. Technol., **124**, 97–103 (2000)
8. L. García-González, M. G. Garnica-Romo, J. Hernández-Torres and F. J. Espinoza-Beltrán, Braz. J. of Chemical Eng., **24,** 2, 249–257 (2007)
9. H. C. Barshilia, K. Yogesh, K.S. Rajam, Vacuum, **83**,427–434 (2009)

10. T. M. Cholakova, V. A. Chitanov, L. P. Kolaklieva, R. D. Kakanakov, D.G. Kovacheva, P. K.Stefanov, S. N. Rabadzhiyska, E. A. Korina, V. I. Kopanov, Bulg. Chem. Commun, **48**, Spec. Iss. 384 – 390 (2016)
11. P.L. Tam, Z.F. Zhou, W. Shum, K.Y. Li, Thin Solid Films, **516,** 5725-5731 (2008)
12. G.S. Fox-Rabinovich ,A.I. Kovalev, M.H. Aguirre, B.D. Beake, K. Yamamoto, S.C. Veldhuis, J.L. Endrino, D.L. Wainstein, A.Y. Rashkovskiy, Surf. & Coat. Technol., **204**, 489–496 (2009)
13. H. Zhou, J. Zheng, B. Gui, D. Geng, Q. Wang, Vacuum **136,** 129-136 (2017)
14. Oliver, W.C.; Pharr, G.M., J. Mater. Res. **7,** 1564-1583 (1992)
15. M. S. Kabir, P. Munroe, Z. Zhou, Z. Xie, Surf. & Coat. Technol. **309**, 779–789 (2017)
16. Y. Shi, S. Long, S. Yang, F. Pan, Appl. Surf. Sci. **254,** 7342–7350 (2008)
17. L. Lu, Q. Wang, B. Chen, Y. Ao, D. Yu, C. Wang, S. Wu, K. Ho Kim, Trans. Nonferrous Met. Soc. China, **24,** 1800−1806 (2014)
18. G. Mishev, V. Rupetsov, S. Dishliev, Ch Pashinski., *11th International Conference in Manufacturing Engineering Proceedings*, 1-3 October 2014, Thessaloniki, Greece, 139-147 (2014)
19. V. S. Rupetsov, J. of Food and Pack. Sci., Technique and Technologies, **1,** 4, 60-65 (2014)